

Neutron Flux Calculation for BNCT with Monte Carlo-Diffusion Hybrid Method

Chang-Min Lee^a, Nam-Suk Jung^b, Hee-Seock Lee^{a,b*}

^aDivision of Advanced Nuclear Engineering, POSTECH, Pohang 37673, Republic of Korea

^bPohang Accelerator Laboratory, POSTECH, Pohang 37673, Republic of Korea

*Corresponding author: lee@postech.ac.kr

1. Introduction

Boron Neutron Capture Therapy (BNCT) is a kind of radiation treatment that uses B(n, α)Li reaction. Since α particle and Li ion have a short range in human body, most of the energy is deposited on the point where the reaction occurs. Epithermal neutron that has energies from several keV to 10 keV is used to maximize the thermal neutron flux in the inner tissue.

To calculate dose distribution in a human body, accurate Boron-10 distribution and neutron flux are needed. Generally, neutron flux can be obtained by the Monte Carlo calculation. On the other hand, there have been some attempts to apply multigroup diffusion equation to BNCT neutron flux calculation to minimize the calculation time [1]. However, multigroup diffusion equation is inaccurate when it uses fewer energy groups. As the number of energy groups increases, it loses the relative time advantage compared to the full Monte Carlo calculations. Therefore, this paper suggested the hybrid model to improve the calculating speed.

2. Methods

The mechanism of Monte Carlo-Diffusion Hybrid Method is introduced. The FLUKA is used for the Monte Carlo code and the DIF3D is used for the three-dimension diffusion code [2,3]. In addition, the correction methods of the diffusion code are suggested by considering the characteristic of heterogeneous head phantom.

2.1 Monte Carlo – Diffusion Hybrid Method

When an epithermal neutron enters the water phantom, neutron loses its own energy rapidly and becomes a thermal neutron. Thus, thermal neutron transport takes most of the time in Monte Carlo calculation. Relatively a less time is spent to calculate the slowing-down process of epithermal neutrons. With these characteristics, this paper suggests Monte Carlo-diffusion hybrid method that calculates the neutron transport at epithermal energy (more than 0.2 eV) with Monte Carlo code and calculates one at thermal energy (less than 0.2 eV) with one group diffusion. In this hybrid model, every scattering position that neutron becomes under 0.2 eV energy is recorded as the fixed-source of thermal neutron.

When higher energy neutron enters the material containing hydrogen, neutron becomes thermal equilibrium state rapidly. Because every elements in human body has high scattering cross section compared to absorption cross section, lots of neutron scattering

occur before neutrons exit the phantom or are captured by other material. In the Monte Carlo code, scattering probability and positions are calculated whenever neutron has scattering event. Therefore, the Monte Carlo code consumes a lot of computing time to calculate thermal equilibrium neutron transport.

To check the ratio of calculation time for epithermal neutron and thermal neutron, we set two kinds of FLUKA input files and execute them. 1) 10 keV monoenergy epithermal neutron enters to 20×20×20 cm³ water phantom. The shape of neutron beam is uniform annular that has radius 7.5 cm. There are no cutoffs for neutron but electron and photon are neglected. 2) The same condition with previous input file except the neutron cutoff of 0.2 eV is set for neutron. Both input files calculate neutron flux. For the comparison, the number of primaries are the same for both input files. i7-8786K CPU is used and 10 cores are activated.

Table 1. Calculation time comparison between two different input files. Other parameters are the same except neutron cutoff

	No Cutoff	0.2 eV Cutoff
Primaries	5×10 ⁷	5×10 ⁷
Calculation Time	522 seconds	98 seconds

It is found from Table 1 that the Monte Carlo code consumes more than 80% for calculating thermal neutron transport, and less than 20% for calculating epithermal neutron transport.

2.2 FLUKA

The FLUKA is a multi-purposed Monte Carlo code. It has been used widely for radiation shielding calculations, irradiation, dosimetry and radiation therapy. [2]. In the FLUKA, a neutron transport is divided to two energy ranges; above 20 MeV and less than 20 MeV. The lower energy neutrons are divided by 260 energy groups from 1E-11 MeV to 20 MeV. For the major human body elements like H, C, N, O, and Ca, the group neutron library is based on recent versions of several evaluated nuclear data.

FLUKA user routine can record individual particle condition like energy, particle type and secondary particle generation. We set user routine to check every point that neutron becomes thermal neutron that lower than 0.2 eV. This neutron is discarded to finish the

calculation after saving the position of thermal neutron generated.

2.3 DIF3D

DIF3D is three-dimension finite difference method (FDM) code, developed by Argonne Nation Laboratory. This code is used for nuclear reactor neutron flux calculation. It supports multigroup diffusion for fixed neutron source or fission source. It can also be used for calculating flux in phantom [4]. Since it has limitation for calculating heterogeneous human body, modified DIF3D code that contains some corrections that explained in section 2.5 and 2.6. Our hybrid method needs only one diffusion group because DIF3D will calculate only under 0.2 eV neutrons.

In mesh-centered DFM, balance equation of one individual cell can expressed as following equation.

$$-\sum_{p=1}^6 \bar{J}_l^p A_l^p + \Sigma_l^r \bar{\varphi}_l V_l = \bar{Q}_l V_l \quad (1)$$

where the \bar{J}_l^p is the surface-averaged net neutron current, A_l^p is the area of surface p , Σ_l^r is the macroscopic absorption cross section, V_l is volume of cell and \bar{Q}_l is cell-averaged fixed source. \bar{Q}_l is calculated by FLUKA (section 2.2).

To solve net neutron current, one assumption is needed; the flux varies linearly from the center of the mesh cell to the midpoints of any of its six surfaces. With this assumption, net neutron current \bar{J}_l^p can be expressed with flux difference between neighboring cells l and m .

$$\bar{J}_{lm}^x = \frac{1}{\Delta x_i/2D_l + \Delta x_{i+1}/2D_m} (\bar{\varphi}_l - \bar{\varphi}_m) \quad (2)$$

Where Δx_i and Δx_{i+1} are length of cell for x axis and D is diffusion coefficient.

2.4 Effective Cross Section Calculation with Water-equivalent Phantom

One group diffusion equation needs two input parameters; macroscopic absorption cross section Σ_l^r for Eq. 1 and diffusion coefficient D for Eq. 2. Since there is an unknown effective neutron spectrum in a single group for diffusion equation, effective diffusion coefficient and absorption cross-section for every major element (H, C, N, O, and Ca) are calculated by gradient descent fitting with DIF3D result and FLUKA result. This method is based on this paper [4].

Calculated scattering and absorption cross-section are as shown in Table 2.

Table 2. Calculated effective scattering and absorption cross-section

Element	Scattering Section (barn)	Cross Section (barn)	Absorption Section (barn)	Cross Section (barn)
H	31.6810		0.28770	
C	7.29445		0.00597	
N	13.5400		1.59098	
O	5.25598		0.00026	
Ca	3.14752		0.56569	

Figure 1 shows validation result, comparison between FLUKA only and hybrid method, with optimized cross sections. 7.5 cm radius annular neutron beam enter $20 \times 20 \times 20 \text{ cm}^3$ water phantom in a z direction. 10 keV monoenergy neutron is used.

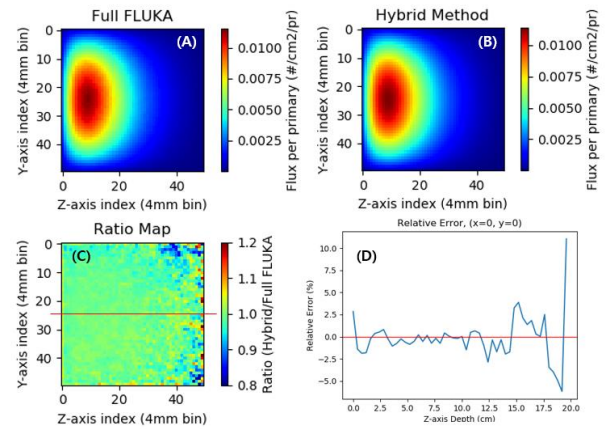


Fig. 1. Calculation result of water phantom with neutron beam incidence. (A) Thermal neutron flux at $x=0$ plane with full FLUKA calculation. (B) Thermal neutron flux at $x=0$ plane with hybrid method. (C) Ratio map B/A (D) 1D flux relative error between (A) and (B) at $x=0, y=0$ line.

2.5 Modified DIF3D and Correction Methods

Original DIF3D code has some limitations. Because the original purpose of this code is for reactor analysis, it cannot make a reasonable result to small and complicate structure like human body. Void region inside of human body like nasal cavity is one of the critical problem. It makes big difference between Monte Carlo calculation and diffusion code. Therefore, this paper uses two correction methods to solve these problems.

2.5.1 Coarse Boundary Correction

When the structure that has curved surface is converted to Cartesian voxel model, surface area is overestimated than original surface. Therefore, diffusion code will overestimate neutron leakage at the surface cell. This problem is not critical in the simple geometry like cubic water phantom. However, in the case of complicated phantom like human body, this problem can be critical. The algorithm of surface area estimation is

implemented and it is used for coarse boundary area correction [5].

2.5.2 Inner Boundary Correction

Diffusion equation makes big error if neutron scattering mean-free-path is much larger than voxel size. In this situation, neutron do not take multiple scattering in a one cell and cannot take diffusion characteristic. Head phantom has empty space that contains air, instead of tissue like oral cavity and nasal cavity. If these cells are assigned with air and take diffusion method, these cells will cause a big error.

To correct this problem, this paper suggest some correction techniques based on isotropic neutron transport in vacuum. Since neutron scattering does not occur in vacuum, neutron moves from the original cell to other cells in a straight line. The probability of neutron transport between two cells is proportional to solid angle.

In inner boundary correction, every voxel that has low density (oral cavity and nasal cavity) is set to inner vacancy cell. Every neighboring material cell is set to inner boundary cell. Ray tracing algorithm find every candidate cell that neutron do not make collision in a path. Real area product geometric factor becomes effective area.

Balance equation is modified from Eq. 1 to Eq. 3.

$$-\sum_{p=1}^6 \sum_{n=1}^{n_{max}} \bar{J}_l^p A_l^{pn} + \sum_l \bar{\phi}_l V_l = \bar{Q}_l V_l \quad (3)$$

Where n_{max} is number of cell that ray can reach from surface p to cell n and A_l^{pn} is effective area between surface p and cell n. It is calculated by geometric factor (solid angle). $\sum_{n=1}^{n_{max}} A_l^{pn}$ should be same with A_l^p

3. Results

3.1 CT Based Head phantom neutron flux calculation

For testing real head phantom model, this study uses voxel model that converted from CT data. Voxel model has $4 \times 4 \times 4$ mm³ cell size. Hounsfield-material conversion table is from FLUKA DICOM module. CT data is from sample data in 3D Slicer code [6]. CT data is acquired by Kingston General Hospital in 2017. Patient information is not released. Calculation result is shown in Figure 2. Like fig. 1, annular neutron beam that has 7.5 cm radius and 10 keV monoenergy.

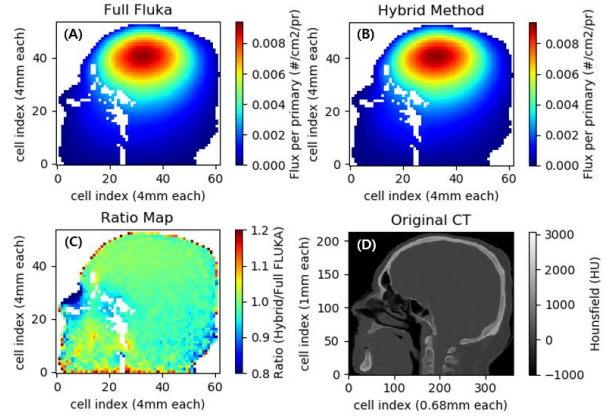


Fig. 2. Calculated result with epithermal neutron beam (A) Thermal neutron flux at the sagittal plane with full FLUKA calculation. (B) Thermal neutron flux at the sagittal plane with hybrid method. (C) ratio map B/A (D) Original CT image at the sagittal plane

The calculation time comparison between full the FLUKA calculation and Hybrid Method are as shown in Table 3. To compare these methods in same environment, both methods uses same number of neutron primaries in FLUKA part. i7-8786K CPU is used and 10 cores are activated.

Table 3. Calculation time comparison between the full FLUKA calculation and hybrid method

Calculation Method	Full FLUKA Calculation	Hybrid Method
Primaries	10 ⁸	10 ⁸
Total Calculation Time	80 minutes	33 minutes
FLUKA part Calculation time	80 minutes	32 minutes

The mean relative difference between flux distribution calculated by only FLUKA and by this hybrid method was 1.89%. Total calculation time reduced from 80 minutes to 33 minutes. Hybrid method can reduce to 60% of total calculation time. In a case of water phantom, calculation time is reduce to 80%. Because of hydrogen density difference between water and tissue, the reduction effect of calculation time in water phantom is larger than in CT based head phantom. Hydrogen can thermalize the epithermal neutron with a few scattering than other material.

3.2 Advantages of DIF3D correction methods

Figure 3 shows the necessity of coarse boundary correction and inner boundary correction. Without these, lots of error occurred around the boundary. Every image on Figure 4 shows the ratio like Fig. 3-(C). These images compare the ratio between full FLUKA calculation and hybrid method that using correction or not.

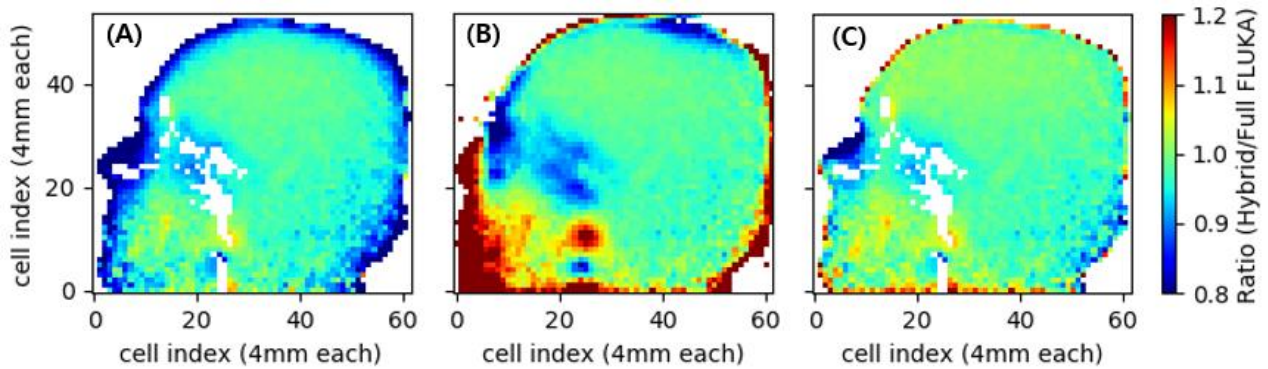


Fig. 3. Calculated result with heterogeneous head phantom epithermal neutron beam. Every figure shows the ratio of hybrid method and full FLUKA calculation. (A) Only inner boundary correction is used. (B) Only coarse boundary correction is used. (C) Both correction methods are used

3. Conclusions

In this work, Monte Carlo-diffusion hybrid method was investigated. In a test case of CT based head phantom, the mean relative difference between flux distribution calculated by only FLUKA and by this hybrid method was 1.89%. The hybrid method could reduce to 60% of total calculation time compared to the full FLUKA calculation. In an IMRT guideline, the accepted difference level between the calculated point dose and the measured dose should be less than 3%. Therefore, this hybrid method with difference of 1.89% is available to be applied for the flux distribution calculation of the BNCT treatment. More investigations that include dose conversion will be performed soon.

REFERENCES

- [1] TAKADA, Kenta, et al. Development of Monte Carlo based real-time treatment planning system with fast calculation algorithm for boron neutron capture therapy. *Physica Medica*, 2016, 32.12: 1846-1851.
- [2] FERRARI, Alfredo, et al. FLUKA: a multi-particle transport code. Stanford Linear Accelerator Center (SLAC), 2005.
- [3] Derstine, K. L. DIF3D: A code to solve one-, two-, and three-dimensional finite-difference diffusion theory problems. No. ANL--82-64. Argonne National Lab., 1984.
- [4] ALBERTSON, B. J.; BLUE, T. E.; NIEMKIEWICZ, J. An investigation on the use of removal-diffusion theory for BNCT treatment planning: A method for determining proper removal-diffusion parameters. *Medical physics*, 2001, 28.9: 1898-1904.
- [5] LINDBLAD, Joakim. Surface area estimation of digitized 3D objects using weighted local configurations. *Image and Vision Computing*, 2005, 23.2: 111-122.
- [6] KIKINIS, Ron; PIEPER, Steve D.; VOSBURGH, Kirby G. 3D Slicer: a platform for subject-specific image analysis, visualization, and clinical support. In: *Intraoperative imaging and image-guided therapy*. Springer, New York, NY, 2014. p. 277-289.